MAGNETIC CONFINEMENT

TOKAMAK CODE TOKES: MODELS AND IMPLEMENTATION

I.S. Landman

Karlsruhe Institute of Technology (KIT), Institute for Pulsed Power and Microwave Technology, P.B. 3640, 76021 Karlsruhe, Germany

The code TOKES was recently developed aiming at integrated simulation of plasma equilibriums and surface processes in tokamaks. Main features of TOKES are described. The code calculates processes in multi-fluid plasma and neutral atoms in the vessel, including plasma heating by neutral beams, transport of hot plasma and electromagnetic radiation, and surface responses to the load, such as the sputtering and the vaporization. The magnetic field is also addressed.

PACS: 52.40Hf

1. INTRODUCTION

So far, the most advanced fusion concept bases on the tokamak magnetic trap in which deuterium and tritium (DT) burn. Efficient personal computers made possible to install a virtual tokamak on many working desks for joint design elaborations of real tokamaks. For example the code ASTRA [1] implements a joint platform for confined tokamak plasma itself. The code TOKES ('Tokamak Equilibrium and Surface processes') follows this way expanding the modeling for the whole tokamak vessel.

TOKES models keep the toroidal symmetry as a basic feature of tokamak principle. The code simulates plasma evolution in time t describing it with diverse functions, such as plasma pressure $p(t,r,z)$, of main cylindrical coordinates, r and z, or in magnetic flux coordinates. The plasma slowly changes equilibrium with the confining magnetic field **B**, which occurs due to internal dissipative processes, such as cross-diffusion and variations of external parameters such as the DT inflow. The simulation involves dynamical changes of plasma shape and electric current density **J** as in the plasma as in external coils of poloidal magnetic field (PF coils).

For virtual tokamaks real physics lexicon can naturally be used. Thus TOKES steadily 'creates' hot plasma by fuelling the core with DT atoms. The fusion reaction produces helium ions, fast neutrons, and the heat. Impurities from the wall contaminate the plasma. The code simulates core impurities in the way it does for the main species, with a common multi-fluid plasma model. The plasma diffuses across nested magnetic surfaces. Then it passes the scrape-off layer (SOL) and dumps onto vessel walls. The wall surface absorbs also the electromagnetic radiation from the plasma and the neutrons as well. The surface responses to the impact, backscattering impacting ions and emitting sputtered atoms and, if the load is very large, the vapor of wall material. The erosion products, which are emitted atoms of wall materials, freely propagate in the vessel before having ionized. Whole calculation is split into sub-steps according to the physical processes (splitting method).

There are publications (the last one [2]) that describe TOKES applications, mainly for the future tokamak ITER. A detailed description of TOKES models is available [3]. This work gives a compressed insight into the models. The whole text consists of the sections that describe various features of this integrated two-dimensional approach.

2. MULTI-FLUID PLASMA

MHD equilibrium states are described with the equation $\nabla p = (1/c)\mathbf{J}\times\mathbf{B}$. It follows that p keeps constant on nested magnetic surfaces (surface function). To describe $\mathbf{B} = (B_r,B_z,B_\zeta)$, poloidal components B_r and B_z use poloidal magnetic flux $w(r,z)$: $B_r = (1/r)\partial w/\partial z$ and $B_z = -(1/r)\partial w/\partial r$. The toroidal field $B_\zeta = \omega/r$ with $\omega(t,w)$ a surface function. The plasma is numerically organized as many toroidal finite elements ('cells') along the contours of constant w. From the Maxwell's equations, the Grad-Shafranov equation [4] follows:

$$r\frac{\partial}{\partial r}\left(\frac{1}{r}\frac{\partial w}{\partial r}\right)+\frac{\partial^2 w}{\partial z^2}=-\frac{d}{dw}\left(\frac{\omega^2}{2}\right)-4\pi r^2\frac{dp}{dw}\,. \qquad (1)$$

TOKES solves Eq.(1) using the Green function of the left side [5] and produces w at given $\omega(w)$ and $p(w)$ which are described with plasma transport equations.

The plasma transport is described using orthogonal magnetic flux coordinates (x,y) where x is radial index coordinate (it counts numerical plasma layers when crossing their borders of $w = \text{const}$) and y poloidal index coordinate. Plasma cell's area on the poloidal plane $s = h_x h_y$ with h_x and h_y the corresponding cell sizes, and the cell's volume $G = rs$ per one radian of toroidal angle ζ.

The well known MHD plasma equations [6] give $p(t,w)$ in terms of several ion species i: ion and electron densities n_i, n_e as well as their temperatures T_i, T_e. The electric field **E** in terms of **J** follows also (the Ohm's law) and **J** is again expressed in terms of ω and p. The function ω follows in terms of electric field $\mathbf{E}'$ in (x,y) frame as

$$\frac{\partial}{\partial t}\left(\frac{s}{r}\omega\right)+c\frac{\partial}{\partial x}\left(h_y E'_y\right)-c\frac{\partial}{\partial y}\left(h_x E'_x\right)=0\,. \qquad (2)$$

The equations form a closed system (which is too bulky to present here) describing the processes such as diffusion and ion-ion mixing in the Pfirsch-Schlueter plasma.

Energy transport across **B** is also considered, including the thermal conduction flux $q_{g\perp} = -\kappa_{g\perp}\partial T_g/h_x\partial x$ of a species $(g = i,e)$. It is to note that realistic plasma diffusion coefficients and thermal conductivity $\kappa_{g\perp}$ are rather uncertain. The neoclassical-, Bohm's- and gyro-Bohm's transport models are implemented. For instance, electron gyro-Bohm thermal conductivity of TOKES reads

$$\kappa_{e\perp}^{GB}\approx\frac{1}{32}\left(\frac{2T_e}{m_e}\right)^{3/2}\left(\frac{m_e c}{eB}\right)^2\frac{\partial n_e}{h_x\partial x}\,. \qquad (3)$$

Ions in TOKES can be at different electron states of ionization z and excitation k. The internal energy of not ionized atom m at ground state ($k = 0$) equals zero. The internal energy E_{mzk} of state (z,k) is a sum of ionization potentials I_z and the excitation energy: $E_{mzk} = \sum_{z'} I_{z'} + \Delta E_{mzk}$ ($0 \le z' < z \le Z_m$, $0 \le k \le K_{mz}$) with Z_m the chemical number and K_{mz} the index of maximum excitation state of database.

At the sub-step of plasma transport the internal states do not change. Each (mzk) species diffuses and mixes according to MHD equations averaged on (zk) which provides some ion transport velocities υ_i. Final transport is calculated using the convective equation for each n_{mzk}:

$$\frac{\partial n_{mzk}}{\partial t} + \frac{\partial \upsilon_i n_{mzk}}{h_x \partial x} = 0 \,. \qquad (4)$$

Increasing p can produce MHD instabilities and thus destroy the equilibrium. Those instabilities develop above the Troyon limit $\beta_{\max}$ for the parameter $\beta = 8\pi p/B^2$:

$$\beta_{\max} = 2.8 \times 10^{-2} \frac{I_{[MA]}}{a_{[m]} B_{[T]}} \,. \qquad (5)$$

Here I is plasma current and a plasma minor radius. We introduced some additional factor $f_\beta \propto (\beta/\beta_{\max})^4$ for the plasma diffusivity $D_\perp$ and the thermal conductivities $\kappa_{g\perp}$ due to which the transport increases drastically when β exceeds $\beta_{\max}$. This keeps p below the Troyon limit.

3. MODELLING OF NEUTRALS

The neutrals (atoms, radiation rays and neutrons) travel in straight lines as some rays being unaffected by the magnetic field. Fig.1 demonstrates the poloidal plane projections of the trajectories of rays propagating in the vessel of ITER. The atoms injected as beams or emitted by the wall finally strike the wall. They can also get once ionized through collisions with free electrons. The new ions join the plasma. In TOKES model for plasma heating by the neutral beam (NB) the new fast ions are slowed down in the magnetic layer of their origin. For the wall emitted atoms the Monte-Carlo method is applied. The rays start at the wall surface as many half-isotropic randomized beams.

Ray intensity I obeys the Buger's law $dI/dl = -I/L$, with l the coordinate along atom ray and L the absorption length. The propagation of neutrals through the vessel is assumed to be toroidally symmetric. In particular, real NB is injected through a small window in the surface, but TOKES assumes it to be symmetrically spread over ζ. Due to high thermal velocity of ions, NB produces negligible poloidal non-homogeneity, thus interacting with the plasma like the spread beam.

The flux w, the plasma and the neutrals are available in the whole vessel of arbitrary shape. In Fig.1 the rays are seen as the curves assembled of straight lines across the triangular cells. At the triangles' corners c the values $w = w_c$ are calculated solving Eq.(1) and the flux w linearly interpolated from the values w_c. The contours of $w(r,z)$ = const are then built for the magnetic layers.

The layers contain the plasma as chains of rectangular cells (one cell per contour segment across triangle). This structure enables convenient coupling of neutrals and plasma cells. The layers are ordered as a graph structure through which the plasma diffuses. Special algorithms for cross-transport on the graph have been developed. The graph ordering allows arbitrary profile of $w(r,z)$, in particular many extremes and x–points.

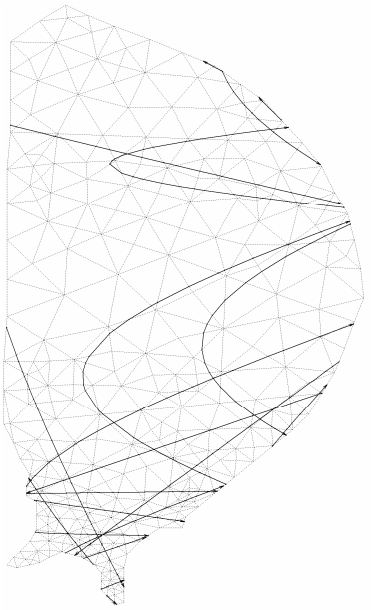

Fig. 1. Poloidal projections of ray trajectories

4. RADIATION TRANSPORT

For ion species m, Eq.(4) calculates transport contribution to $\partial n_{zk}/\partial t$. Following [3,7], the contributions of ionization dynamics and radiation losses are given by

$$\frac{\partial n_{zk}}{\partial t} = S^{ed}_{zk} + S^{ir}_{zk} \,. \qquad (6)$$

The terms describe the excitation- and deexcitation transitions among the levels (S^{ed}) and the ionization and recombination (S^{ir}) of charge states, accounting for the impacts of both photons and free Maxwell's electrons. For example, the term S^{ed} of Eq.(6) reads (omitting z)

$$S^{ed}_k = \sum_{k'=0}^{k-1} \left(\nu^e_{k'k} n_{k'} - \nu^d_{k'k} n_k \right) + \sum_{k'=k+1}^{K} \left(\nu^d_{kk'} n_{k'} - \nu^e_{kk'} n_k \right) . \qquad (7)$$

Electron impact processes are based on the excitation and deexcitation frequencies ν^e and ν^d. For them the detailed balance principle (the Boltzmann's relation) is used:

$$\nu^{\mathrm{Ed}}_l = \nu^{\mathrm{Ee}}_l \left(g_k / g_{k'} \right) \exp\left(\Delta E_l / T_e \right) . \qquad (8)$$

The g_k are level's statistical weights and $\Delta E_l = E_{k'} - E_k > 0$ the transition energy. Similarly, the Saha formula relates the frequencies of ionization and recombination:

$$\nu^{\mathrm{Er}}_{zk} = \nu^{\mathrm{Ei}}_{zk} \left(g_{zk} / g_{z+1,0} \right) \left(n_e / n^S \right) \exp\left(I_{zk} / T_e \right) . \qquad (9)$$

Here $n^S = \frac{1}{4}\pi^{-3/2} (T_e/\mathrm{Ry})^{3/2} / (r_B)^3$ is the Saha density, Ry the Rydberg constant, and r_B the Bohr radius.

The radiation rays are directed randomly, with isotropic distribution. One ray starts from a random point $\mathbf{r}_0$ of a plasma layer uniformly distributed over its volume.

The Buger's law for the photon ray intensity reads $dI/dl = \beta - \kappa I$, with β and κ the opacities corresponding to resonance (line), recombination and Brehmstrahlung kinds of radiation. For instance, line radiation emissivity reads

$$\beta_l = (4\pi)^{-1} A_l L_l(\varepsilon) \Delta E_l n_{k'} . \qquad (10)$$

Here A_l [s^{-1}] is the Einstein coefficient and $L_l(\varepsilon)$ the line shape function. For the Brehmstrahlung, the Maxwell's electrons provide the Kirchhoff's law $\kappa_b'(\varepsilon) = \beta_b(\varepsilon)/I_P(\varepsilon)$, with I_P the Planck's distribution function of photons.

The radiation reabsorption is not yet implemented so far. It is to note that the dielectronic recombination was simulated in a simplified way increasing photoionization cross-section by some factors $F_{DR}(m,z)$, which seems acceptable as long as reabsorption of recombination radiation is not accounted for.

A database for basic atomic parameters such as ΔE_{mzk}, A_{mzl}, g_{mzk}, I_{mz}, and the cross-sections of excitations and ionizations is available. Only necessary populations for n_{mzk} are calculated, with some ranges $z_{1m} \le z \le z_{2m}$ for ion charges and $0 \le k \le K_{mz}$ that vary over the plasma layers being updated after each time step t_j. Integration of Eq. (6) is done for each plasma layer using the implicit finite-difference scheme of type

$$\mathbf{n}(t_j) - \mathbf{n}(t_{j-1}) = \nu(t_{j-1})\mathbf{n}(t_j)(t_j - t_{j-1}) . \qquad (11)$$

Here $\mathbf{n}$ is the vector of n_{mzk} and ν the frequency matrix. A stable algorithm for the effective solution of Eq.(11) with arbitrary time steps is developed.

For validation of the radiation model we used the radiation parameter, R, and ion mean charge produced by D. Post [8] as dependencies on T_e. The code calculates the total radiation power P_{rad} from one plasma cell and divides it by the product of electron and atom densities $n_e n_m$, which gives R. Fig.2 shows such comparisons in case of tungsten impurity (m = W) in hydrogen plasma. The radiation due to H-ions is not subtracted, but n_H is taken small enough for neglecting the contribution of H.

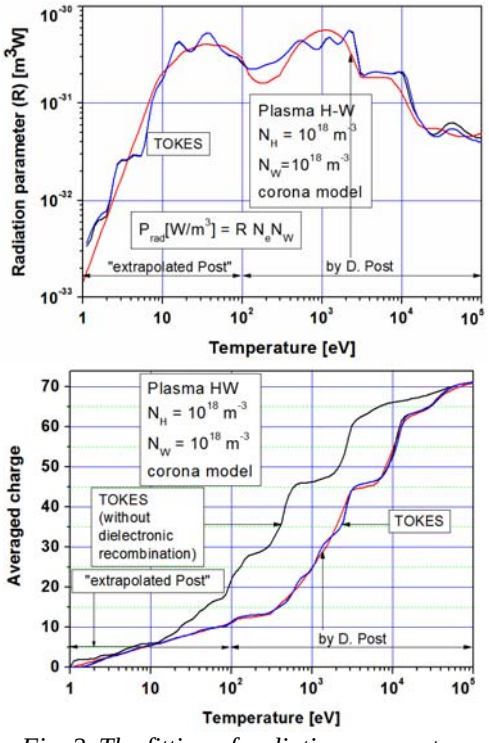

Fig. 2. The fitting of radiation parameter and mean charge state for tungsten

The 'visually acceptable' fitting between Post's data and TOKES results was achieved after some tuning up of the collision excitation frequencies and the factors $F_{DR}(m,z)$. The fitting factors were found after many comparisons and testing of different values. So far, the validation was also done for He to C, Ne and Ar.

In Fig. 2 the 'extrapolated Post' means that appropriate reference data is not available, thus for T_e < 100 eV TOKES results only are actually shown.

5. VESSEL WALL PROCESSES

Surface processes backscattering, vaporization and physical sputtering are implemented, simulating the emission of atoms due to the impacts of energetic particles. In theory we follow the review [9].

The sputtering is described with the sputtering yield Y, which is averaged number of emitted atoms per one incident particle; Y depends on the incident energies E. Target atom can after impact leave the surface if its energy exceeds the surface binding energy E_S. For the materials to be used in ITER, which are beryllium (E_S = 3.38 eV), graphite (E_S = 7.42 eV) and tungsten (E_S = 8.68 eV), TOKES uses the experimental dependences $Y(E)$ from [10]. If some of needed sputtering data is not available there, an analytical model is used. The sputtering yields Y are shown in Fig. 3.

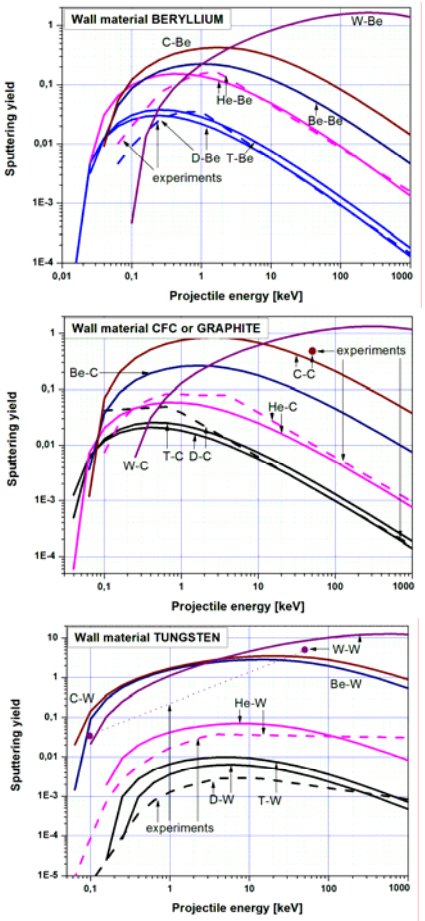

Fig. 3. Sputtering yields for Be,C and W

The numbers N_a and energies E_a of the atoms to be emitted from wall segment of surface area S are in advance accumulated as data pairs (N_a, N_aE_a), separately for the scattered, sputtered and vaporized atoms. When N_a exceeds some given minimum value, or the accumulation period exceeds some given maximum time, the next rays of N_a atoms in the ground state of their bound electrons and with kinetic energy E_a per atom are produced being randomly (half-isotropic) distributed.
The corresponding data pair is then zeroed, and a new accumulation cycle starts. The values of N_a and N_aE_a should be as small as computer speed allows (presently $N_a = 10^{17}$ and $N_aE_a = 1$ J are chosen).

In the wall bulk thermal transport from the surface through the armor material to some cooling equipment is simulated for the bulk temperature $T(t,x)$ with the thermal conductivity equation along the depth x:

$$c\frac{\partial T}{\partial t} = \frac{\partial}{\partial x}\left(k\frac{\partial T}{\partial x}\right) + Q, \quad k\frac{\partial T}{\partial x}\bigg|_{x=0} = -q_0 . \quad (12)$$

The heat capacity c and the thermal conductivity k of the material are some given functions of T. The volumetric heating term Q foresees that some part of wall load energy can be deposited in the bulk, for instance being the stopping power of fast electrons. The other part of load is applied as the surface heat flux q_w, so that $q_0 = q_w$.

The number of material atoms vaporized during time step, N_{vap}, is calculated when q_w is so large that surface temperature would exceed the temperature T_v of the saturation vapor pressure of 1 bar. In this case the boundary condition $T|_{x=0} = T_v$ replaces that of Eq.(12), and we get $N_{\mathrm{vap}} = (q_w - q_0)S\tau/E_{\mathrm{subl}}$, with E_{subl} the sublimation energy, τ the time step and q_0 following from Eq.(12).

6. CALCULATION OF MAGNETIC FLUX

The poloidal magnetic flux $w(\mathbf{p})$ determines plasma shape; $\mathbf{p} = (r,z)$. w is a sum of internal field generated by plasma current J_ζ and the applied field produced by the PF coils. Plasma cell currents through each triangle i (see Fig. 1) are approximated by one current I_i flowing in a thin ring through the triangle's centre $\mathbf{p}_i^{(c)}$. The mentioned Green function, $G(\mathbf{p},\mathbf{p}_i^{(c)})$, produces the field of the ring carrying unit current. The whole flux $w(\mathbf{p})$ is given by

$$w(\mathbf{p}) = \sum_n I_n G(\mathbf{p},\mathbf{P}_n) + \sum_i I_i G\left(\mathbf{p},\mathbf{p}_i^{(c)}\right). \quad (13)$$

The coil currents I_n are approximated by the current rings at some fixed points $\mathbf{P}_n$; I_n are calculated for given I_i.

To keep the plasma off the wall the updating of I_n is dynamically done. For the feedback control in ITER simulations a special technique is developed for 6 PF coils: 1) fixed positions $\mathbf{p}_{x0}$ and $\mathbf{p}_{x1}$ for two x-points are chosen; 2) the confined plasma is assumed be bounded by the separatrix $w(\mathbf{p}) = w_{x0} \equiv w(\mathbf{p}_{x0})$; 3) another separatrix $w(\mathbf{p}) = w_{x1} \equiv w(\mathbf{p}_{x1})$ locates outside the plasma and a small difference $\Delta w = w_{x0} - w_{x1}$ is fixed; 4) some fixed positions $\mathbf{p}_{cj}$ for several points near the vessel surface are chosen where the plasma can touch the wall most probably; 5) the point $\mathbf{p}_{cj\max}$ of maximum value of $w(\mathbf{p}_{cj})$ obtained with the available I_i and previous I_n is used for calculation of new I_n from the condition $w(\mathbf{p}_{i\max}) = w_{x1}$. Thus the code tries to keep the outer separatrix $w(\mathbf{p}) = w_{x1}$ near the wall and therefore the plasma at some distance from the wall.

These conditions determine I_n completely. The newly calculated I_n influence plasma shape and thus the plasma currents I_i. Therefore for final solution several iterations are required. This technique can provide the convergence on a wide range of plasma current profiles.

Fig. 4 demonstrates one of TOKES results obtained for $J_\zeta \approx 0.7$ MA/m^2. The PF coils are displayed with small squares, and calculated values of I_n are indicated nearby.

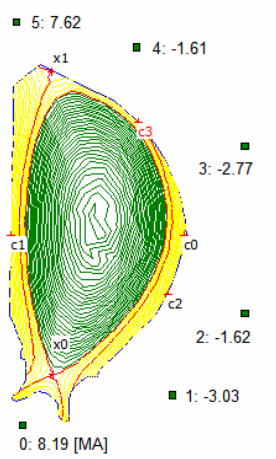

Fig. 4. Magnetic layers $w(\mathbf{p}) = const$

7. CONCLUSIONS

Recently developed integrated tokamak code TOKES is described. The magnetic field can evolve together with the confined plasma and electric currents updated after each time step. The Pfirsch-Schlueter multi-fluid plasma model for ion species is implemented. The fluids are from hydrogen isotopes to tungsten multi-charged ions of bound electron excitation states. This allowed full radiation transport model that includes calculations of level populations. The fluxes of neutrals (atoms, neutrons and photons) propagating through the vessel are simulated based on the Monte-Carlo model with toroidally symmetric big particles ('rays'). The magnetic surfaces are built in the whole vessel volume. Wall processes including surface sputtering and evaporation as well as bulk heat transport are implemented.

TOKES cannot yet be introduced as some finished integrated tokamak code. Its capabilities are not yet acquired mature stage. More work is needed for further development of the code in order to reach reliable integrated modeling.

ACKNOWLEDGEMENTS

I gratefully acknowledge numerous contributions of G. Janeschitz, S. Pestchanyi and R. Kochergov for the development of TOKES concept. Some of algorithms of the code FOREV, the predecessor of TOKES, are used.

This work, supported by the European Communities under the EFDA Task Agreement WP10-PWI between

EURATOM and Karlsruhe Institute of Technology, was carried out within the framework of the European Fusion Development Agreement. The views and opinions expressed herein do not necessarily reflect those of the European Commission.

REFERENCES

1. G.V. Pereversev et al. // *ASTRA: Rep. IPP 5/42* / Max-Planck-Institute für Plasmaphysik, Garching. 1991.
2. I.S. Landman et al.// *Fusion Eng. Des.* 2010, doi:10.1016/j.fusengdes.2010.03.044.
3. I.S. Landman. Tokamak code TOKES models and implementation // *Report of Forschungszentrum Karlsruhe, FZKA-7496.* 2009.
4. V.D. Shafranov // *Reviews of Plasma Physics*. New York: "Consultants Bureau", 1966, v. 2.
5. L.D Landau, E.M. Lifshitz // *Course of theoretical physics*. Oxford: "Butterworth-Heinemann". 2000, v. 8.
6. S.I. Braginskij//*Reviews of Plasma Physics*. New York: "Consultants Bureau". 1965, v. 1.
7. I.S. Landman, G. Janeschitz // *J. Nucl. Mater*. 2009, v. 386–388, p. 915–918.
8. D.E. Post et al.// *Atomic Data and Nuclear Data Tables*. 1977, v. 20, p. 397.
9. D. Naujoks. *Plasma-Material Interaction in Controlled Fusion*. Springer Series on atomic, optical, and plasma physics. Springer-Verlag, Berlin, Heidelberg, 2006.
10. H.H. Andersen, H.L. Bay. Sputtering Yield Measurements // *Topics in Applied Physics* / Springer-Verlag, 1981, v. 47, p.145-218.

Article received 13.09.10

ТОКАМАК КОД ТОКЕС: МОДЕЛИ И РЕАЛИЗАЦИЯ

И.С. Ландман

Недавно разработанный код ТОКЕС предназначен для объединенного моделирования плазменного равновесия в токамаке и процессов на поверхности стенки вакуумной камеры. Описаны основные свойства кода. ТОКЕС рассчитывает физические процессы в многожидкостной плазме и нейтральные атомы в камере, включая нагрев плазмы нейтральными пучками, перенос плазмы и электромагнитного излучения, а также реакцию стенки на нагрузку: атомное распыление и испарение. Магнитное поле также рассмотрено.

ТОКАМАК КОД "ТОКЕС": МОДЕЛІ І РЕАЛІЗАЦІЯ

І.С. Ландман

Нещодавно розроблений код "ТОКЕС" призначений для об'єднаного моделювання плазмової рівноваги в токамаці і процесів на поверхні стінки вакуумної камери. Описано основні властивості коду. ТОКЕС розраховує фізичні процеси в багаторідинній плазмі і нейтральні атоми в камері, включаючи нагрів плазми нейтральними пучками, перенос плазми й електромагнітного випромінювання, а також реакцію стінки на навантаження: атомне розпилення і випар. Магнітне поле також розглянуто.